Applied Surface Science 351 (2015) 119–124

Contents lists available at ScienceDirect

Applied Surface Science

journal homepage: www.elsevier.com/locate/apsusc

Interfacial composition and adhesion of sputtered-Y_2O_3 film on ZnS substrate

Pei Lei[a], Bing Dai[a], Jiaqi Zhu[a,*], Gui Tian[b], Xiaoting Chen[c], Yongshuai Wang[d], Yuankun Zhu[e], Gang Liu[f], Lei Yang[a], Jiecai Han[a]

[a] Center for Composite Materials, Harbin Institute of Technology, P.O. Box 3010, Yikuang Street 2, Harbin 150080, China
[b] Shanghai Institute of Space Propulsion, Shanghai 201112, China
[c] Key Laboratory for Liquid-Solid Structural Evolution and Processing of Materials (Ministry of Education), School of Materials Science and Engineering, Shandong University, Jingshi Road 17923, Jinan 250061, China
[d] Institute of Electronic Engineering, China Academy of Engineering Physics, Mianyang 621999, China
[e] School of Materials Science and Engineering, University of Shanghai for Science & Technology, Shanghai 200093, China
[f] Center for High Pressure Science and Technology Advanced Research, Shanghai 201203, China

ARTICLE INFO

Article history:
Received 29 March 2015
Received in revised form 18 May 2015
Accepted 19 May 2015
Available online 27 May 2015

Keywords:
Magnetron sputtering
Y_2O_3/ZnS interface
XPS depth profile
Nano-scratch measurement
Adhesion

ABSTRACT

Interface engineering has emerged as a fertile and efficacious approach to turn functional properties in the field of film systems. In this work, the interfacial properties of sputtered yttrium oxide films on zinc sulfide substrate (Y_2O_3/ZnS) were analyzed by transmission electron microscopy (TEM), X-ray photoelectron spectrum (XPS) depth profile and nano-scratch measurement. An interface layer with the depth of 20 nm between Y_2O_3 film and ZnS substrate was directly observed by TEM. Under different film growth conditions, although the interfacial features including interfacial width and composition distribution exhibit similar behavior, it is found that higher cohesive strength is obtained under a special substrate bias voltage of −160 V at low substrate temperature. Such an enhanced mechanical property can be understood by the role of physisorbed oxygen in the interfacial region, in which less physisorbed oxygen with van der Waals bonds leads to a strong adhesion. Our results provide a favorable strategy to achieve strong adhesion between oxide and sulfide at low temperature, which are urgent in future micro-electric applications.

1. Introduction

Yttrium oxide [1–7] and zinc sulfide [8–10], possessing multi-functional properties, have been known as the promising materials in a wide range of applications. Interfacing Y_2O_3 and ZnS has been widely used for thin-film electroluminescent devices [11–13], antireflective transmitting windows [14], field emission displays [15] and other functional structures.

Yttrium oxide films were widely fabricated on silicon to build Metal-Insulator-Semiconductor (MIS) devices. The interface between insulator and semiconductor, where charge accumulation and transport occur, has attracted tremendous attention [16–19]. Numerous reports have demonstrated that Y_2O_3/substrate interfacial properties have great impact on the device performance that included but not limited to opt-electron properties [20–22] and thermal conductivity [23]. Nevertheless, the adhesion of coatings to substrate is paramount in practically all application areas [24]. Successful combination and long-term stability of any coated implementation are highly dependent on interfacial adhesion strength between coatings and substrate. Especially, strong cohesion can protect the substrate from the fierce environment when yttrium oxide was used as protective coatings of windows [25,26]. Although the intrinsic structure and properties of Y_2O_3 films have been studied well [5–7] and several methods to improve the metal-oxide adhesion have been reported [24,27], the origin of interfacial and mechanical properties of hetero-materials Y_2O_3/ZnS are really limited and still not fully illuminated.

In this paper, yttrium oxide films were grown on ZnS substrate under different growth conditions to form distinct Y_2O_3/ZnS interfaces. TEM and XPS depth-profile analysis were explored to give detailed information about their interfaces. The adhesion strength was evaluated by nano-scratch measurement and also correlated to the interfacial chemical bonds and structures.

* Corresponding author. Tel.: +86 451 86417970; fax: +86 451 86417970.
E-mail address: zhujq@hit.edu.cn (J. Zhu).

http://dx.doi.org/10.1016/j.apsusc.2015.05.109
0169-4332/

2. Experimental details

Yttrium oxide films were grown on ZnS substrate by radio-frequency magnetron sputtering. In order to detect the interfacial properties controlled by different conditions, the films under different substrate temperatures and bias voltages were synthesized and interfaced to ZnS substrate. The low and high temperatures were 25 °C and 600 °C, and the low and high substrate bias voltages were set as 0 V and −160 V respectively. The other growth parameters remained in the constant state: the power of 130 W, the total pressure of 1.0 Pa, the ratio of Ar:O_2 of 100:4. Before the deposition, resputtering process was applied for all the ZnS substrate to remove the surface contamination and to keep the same surface state for all the samples deposited on. The film thickness was adjusted by deposition time.

In order to prepare the interfacial samples for TEM characterization, ~1.2 μm film on ZnS was cut and fabricated by focused ion beam technique. The TEM images were obtained from TEM equipment (TecnaiF2F30, FEI Corp.) with the accelerated voltage of 300 kV and the line resolution of 0.1 nm. The chemical compositions and bonds were detected by X-ray photoelectron spectroscopy (XPS, Thermo ESCALAB 250) using a monochromatized Al Kα source with a step size of 0.1 eV. The XPS depth-profile analysis was realized by scanning the core level of the Y. O, S and Zn from film surface into substrate. The cohesive strength of Y_2O_3 and ZnS under different growth conditions was evaluated by nano-scratch measurement. The nano-scratch measurement was performed by nano-indenter XP system with force resolution of 100 nN and displacement resolution of 0.5 nm. The procedure was executed as follows: the initial load of 0.1 mN linearly increased to the 100 mN and the distance of tip movement was 1000 μm. The scratch measurement was tested three times for each sample to get more general results.

3. Results and discussions

The TEM images of (~1.2 μm) Y_2O_3/ZnS interface are shown in Fig. 1. Fig. 1(a) exhibits the low-resolution TEM image of interface between ~1.2 μm Y_2O_3 and ZnS substrate. It can be observed that there is a clear and sharp interface instead of an obvious zigzag-shaped transition zone at the scale of 0.5 μm. The film shows the columnar structure and each column is separated by boundaries shown as dark areas. As shown in Fig. 1(b), ZnS substrate contains large grains and in individual ZnS grain the diffraction image exhibits the single crystal feature (cubic, PDF #05-0566). While the films are polycrystalline structure (cubic, PDF #041-1105) as shown in Fig. 1(c). In order to give more details of the interface, the high-resolution TEM was obtained in Fig. 1(d). Unlike the results from regular TEM (Fig. 1(a)), the interfacial boundary between film and substrate is obscure and gradient-like, and a transition zone with ~ 20 nm thickness can be determined.

To further confirm the composition and chemical bonds at the interfacial transition zone, XPS depth-profile was obtained by scanning the surface after every 2 min argon etching. Fig. 2 gives the core level spectra of O1s, Y3d, Zn2p, and S2p under different etching times. As for 0 and 2 min etching, the core level photoelectron spectra of O1s and Y3d have strong intensity as shown in Fig. 2(a) and (b) respectively, verifying the chemical composition of Y_2O_3 films. As the etching time increases, the intensity of O1s and Y3d spectra gradually reduces. While after 12 min etching, O and Y signals are very weak and almost disappear, indicating substrate area has exposed to the detector. In contrast, Zn and S elements show the opposite trend when approaching to the substrate. Before 4 min, there are no signals of Zn and S elements. After 6 min etching, weak peaks of Zn and S appear, and the peaks gradually increase until entering the substrate, which is characterized by the only existed Zn and S peaks. As sputtering deepens from surface into

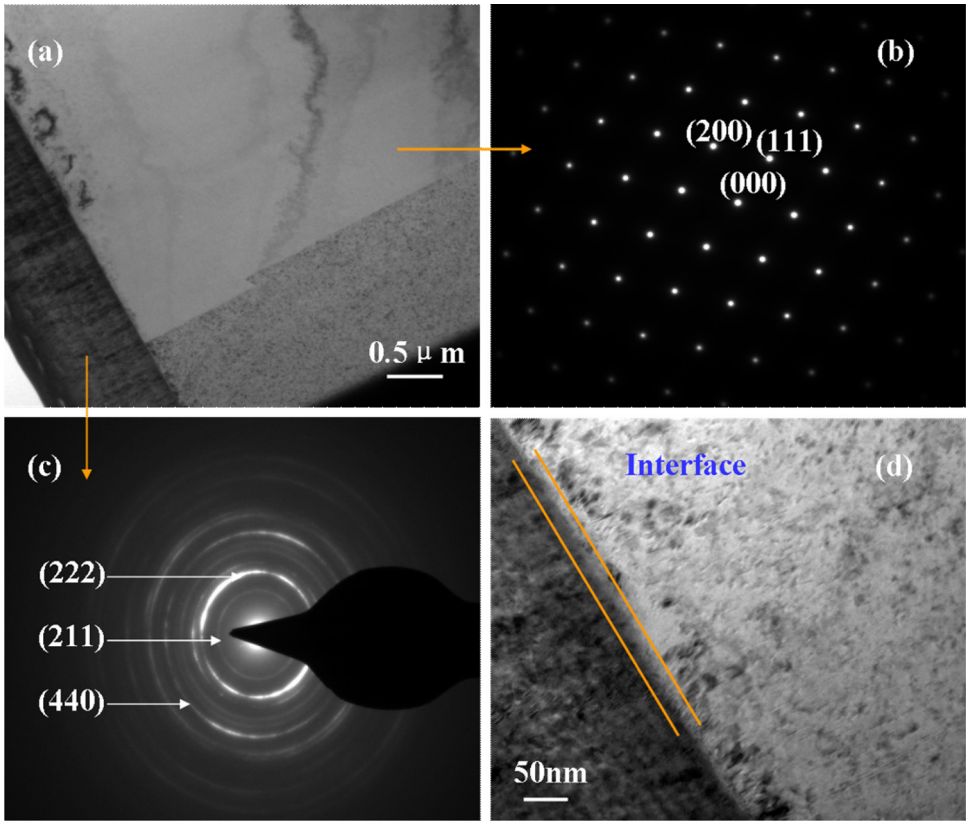

Fig. 1. (a) The low-resolution TEM cross-sectional image of Y_2O_3/ZnS interface; (b) diffraction pattern of one single grain of ZnS substrate; (c) the diffraction pattern of Y_2O_3 film and (d) the high-resolution TEM cross-sectional image of Y_2O_3/ZnS interface (Y_2O_3 film grown on ZnS at 600 °C).

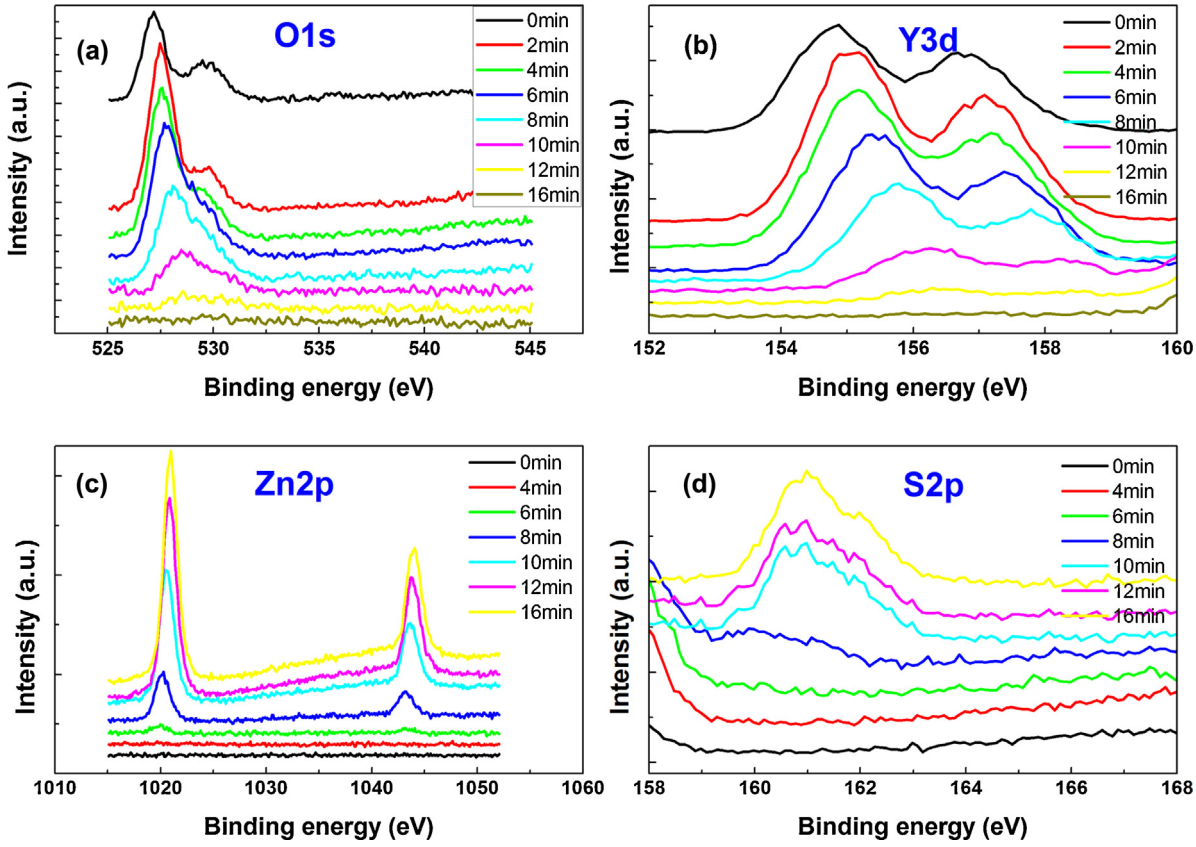

Fig. 2. The XPS depth-profile of (a) O1s, (b) Y3d, (c) Zn2p, (d) S2p of Y_2O_3/ZnS (0 V, 25 °C, ~30 nm Y_2O_3 on ZnS substrate).

substrate, the intensity of all the peaks varies and there are no other peaks appear, indicating the uniform chemical bonds from the surface to the transition zone. It is also observed that there exists the interfacial transition zone which contains four elements within the windows between 6 min and 12 min etching, agreeing well with the TEM images.

Fig. 3 shows the depth-profile of element concentration of Y_2O_3/ZnS interface at substrate voltage of 0 V and −160 V. It is clear to observe the transition zones of Y_2O_3/ZnS interfaces. The elements in Y_2O_3 films are mainly Y and O. After several minutes etching, the transition zone appears, which demonstrates the coexisted Y, O, Zn, and S elements. As the etching time increases, the concentrations of Y and O decrease while Zn and S elements have the reverse trend. The variation of element concentration from the film surface to the substrate was shown in Fig. 3(a) and (b). Although the films were grown in different conditions, it can be observed that the transition zone under the different bias voltages has the similar width.

As shown in Fig. 4, both the element concentration and peak position change as a function of etching time. One can see that O1s peak is deconvoluted into two peaks (at ~529 eV and 531 eV) at Y_2O_3 film surface, corresponding to the Y—O bond and physisorbed oxygen (defined as O_δ) [28]. The O_δ can be mainly attributed to the moisture or contaminations on the surface in the air [29]. While in the films, as the argon ion peels forward and moves into the films, it is believed that the O_δ comes from the injected oxygen gas as well as the same case for interface. Being different with Rubio et al.'s report that the high binding energy of O1s (531 eV) may be related to the carbonate [30], we found that the O_δ greatly varies while the carbon concentration changes slightly in the interface (not shown here). Therefore, it is reasonable to suppose that the dominating

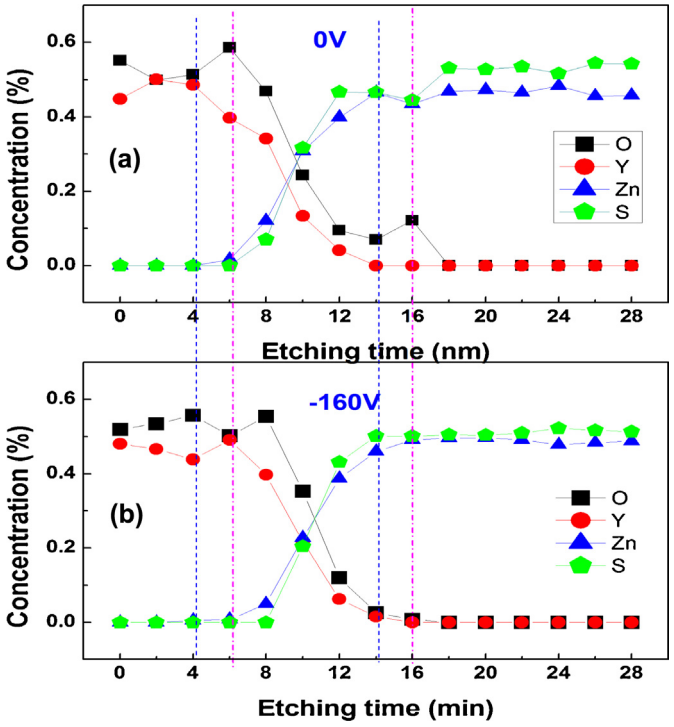

Fig. 3. The depth-profile of element concentration of Y_2O_3/ZnS interface under different film growth conditions of substrate of bias voltage of (a) 0 V and (b) −160 V (25 °C, ~30 nm Y_2O_3/ZnS).

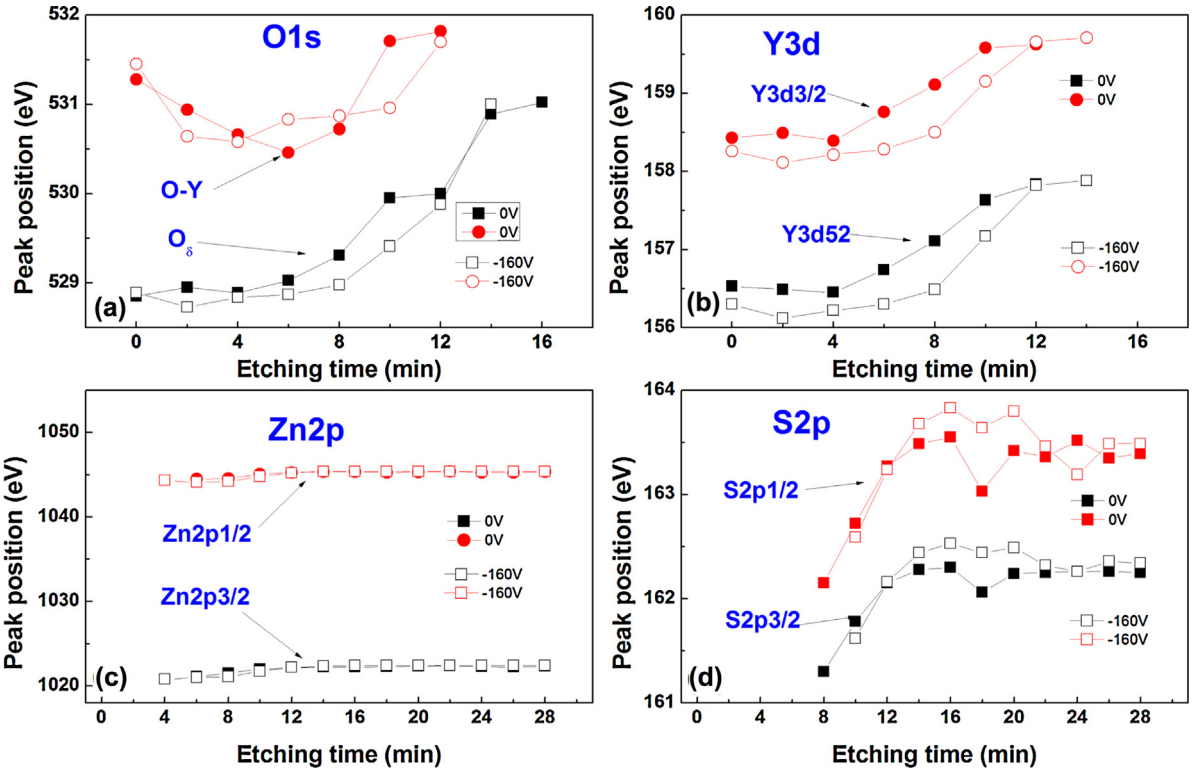

Fig. 4. The variation of peak position of (a) O1s, (b) Y3d, (c) Zn2p and (d) S2p as a function of etching time.

contribution comes from the injected oxygen gas. The Y3d signal can be subdivided into Y3d3/2 and Y3d5/2 peaks due to the spin-orbit coupling [31]. Similarly, both the S2p and Zn2p spectra have two splitting peaks. The positions of both O1s and Y3d move slightly higher position when the probing depth approaches to the interface. However, the positions of Zn2p and S2p move toward low binding energy when approaching to the interface. The results of peak position indicate that there is no other chemical bond formation. Meanwhile, the chemical states of mixed O, Y, S and Zn elements can be modulated by each other, reaching the negotiated states in the interface zone.

To evaluate the cohesive properties of Y_2O_3/ZnS interface under different conditions, the nano-scratch measurement was employed and the results are shown in Fig. 5. As the substrate bias voltage or

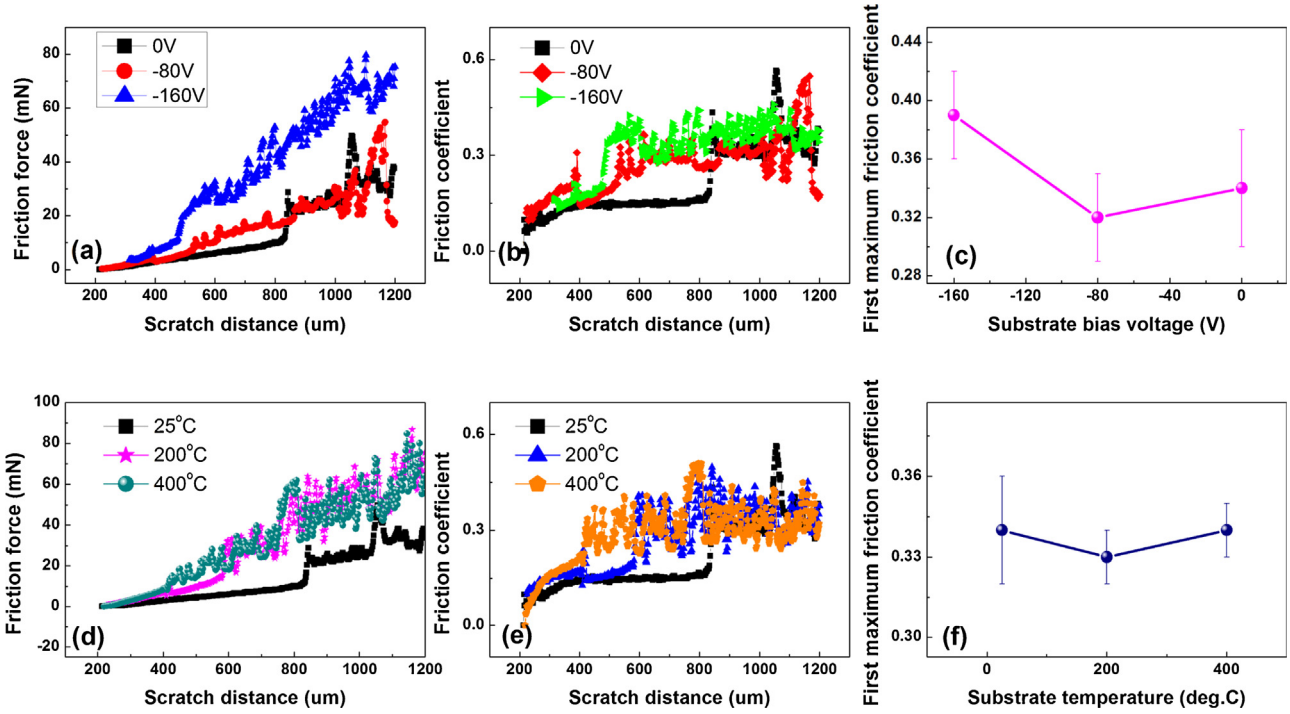

Fig. 5. The friction force and friction coefficient of yttrium oxide films at (a–c) substrate bias voltage of 0 V, −80 V and −160 V, and at (d–f) the temperature of 25 °C, 200 °C and 400 °C.

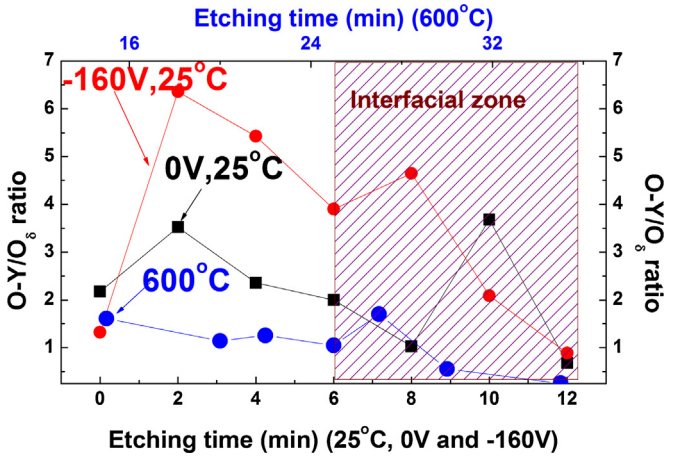

Fig. 6. The ratio of boned O to O_δ(physisorbed O) of Y_2O_3/ZnS interface under three different growth conditions (~50 nm Y_2O_3 film at substrate voltage of −160 V and 0 V, ~120 nm Y_2O_3 films at 600 °C).

substrate temperature increases, the friction force will increase. In order to avoid the influence of thickness on the cohesive properties, the coefficient frictions under different conditions were measured and compared. The first maximum friction coefficient was used to evaluate the cohesive strength. From Fig. 5(c) and (f), the increase in cohesive strength was observed as the substrate bias voltage increases. However, the substrate temperature does not offer an obvious effect. That means the energetic ion bombardment can improve the initial film growth and the interface states during film growth, resulting in the strong cohesive force in the interface. Several researchers also reported the similar results for other material systems [32–35].

In order to explore the influence factor of the cohesive properties between yttrium oxide film and ZnS substrate, we consider the width and chemical bonds of interfacial zone as the main influence factors. We first compare the width of transition zone at different substrate bias voltages as shown in Fig. 3, in which the interfacial width seems to be on the same level. In our work, the same pre-deposition strategy was applied to the same substrate to make sure the same initial surface conditions (i.e. roughness, morphology et al.). Accordingly, the interfacial bond should dominantly contribute the adhesive properties. The higher binding energy of O1s core level is attributed to the physisorbed oxygen. The physisorbed oxygen in the film and interface mainly origins from the occluded gas (inputted oxygen gas) during film deposition. Fig. 6 shows the ratio of boned O to O_δ as a function of etching time. It can be clearly observed that the ratio of boned O to O_δ under bias substrate voltage of −160 V is higher than those of other films in the interface zone. When much O_δ exists in the interface, they reduce the number of strong bonds, resulting in weaker cohesive properties as the bonding of physisorbed oxygen predominately relies on the weak van der Waals forces. Indeed, this bombardment prefers to resputter loosely bonded atoms and implantation [35]. Although the former results showed the less physisorbed oxygen content in yttrium oxide film at higher temperature [28], the higher content of physisorbed oxygen is attributed to the weak cohesion in the interface zone.

4. Conclusion

In order to explore the interfacial features and cohesive properties of Y_2O_3/ZnS, yttrium oxide films were prepared on ZnS substrate under different growth conditions including various substrate temperature and substrate bias voltage. A transition zone with a width of 20 nm was directly observed by high-resolution TEM at Y_2O_3/ZnS interface. Such transition zone can be confirmed by XPS depth-profile analysis, in which the peak position of O1s, Y3d, Zn2p, and S2p change and converge. The nano-scratch measurement demonstrates the bias voltage could enhance the cohesive strength rather than the high substrate temperature. The enhanced Y_2O_3/ZnS interface is mainly attributed to the less physisorbed oxygen (weak van der Waals bonds). Ions interaction is the feasible way to strengthen the interface at low substrate temperature, which is promising for further MEMS application.

Acknowledgement

This work was supported by the National Natural Science Foundation of China (Grant No. 51372053), the National Natural Science Excellent Young Foundation of China (Grant No. 51222205), the Doctoral Program Foundation of the Ministry of Education of China (20112302110036), the Fundamental Research Funds for the Central Universities (Grant NO. HIT.NSRIF.2015040) and the Hei longjiang outstanding youth science fund of China (JC201305).

References

[1] S.B. Liang, Z.Y. Zhang, J. Si, D.L. Zhong, L.M. Peng, High-performance carbon-nanotube-based complementary field-effect-transistors and integrated circuits with yttrium oxide, Appl. Phys. Lett. 105 (2014) 063101.
[2] G.-y. Adachi, N. Imanaka, The binary rare earth oxides, Chem. Rev. 98 (1998) 1479–1514.
[3] M. Zinkevich, Thermodynamics of rare earth sesquioxides, Prog. Mater. Sci. 52 (2007) 597–647.
[4] S.J. Pearce, G.J. Parker, M.D.B. Charlton, J.S. Wilkinson, Structural and optical properties of yttrium oxide thin films for planar waveguiding application, J. Vac. Sci. Technol. A 28 (2010) 1388–1392.
[5] B. Lacroix, F. Paumier, R.J. Gaboriaud, Crystal defects and related stress in Y_2O_3 thin films: origin, modeling, and consequence on the stability of the C-type structure, Phys. Rev. B 84 (2011) 014104.
[6] C.V. Ramana, V.H. Mudavakkat, K.K. Bharathi, V.V. Atuchin, L.D. Pokrovsky, V.N. Kruchinin, Enhanced optical constants of nanocrystalline yttrium oxide thin films, Appl. Phys. Lett. 98 (2011) 031905.
[7] V.H. Mudavakkat, V.V. Atuchin, V.N. Kruchinin, A. Kayani, C.V. Ramana, Structure, morphology and optical properties of nanocrystalline yttrium oxide (Y_2O_3) thin films, Opt. Mater. 34 (2012) 893–900.
[8] X.S. Fang, T.Y. Zhai, U.K. Gautam, L. Li, L.M. Wu, Y.S. Bando, D. Golberg, ZnS nanostructures: from synthesis to applications, Prog. Mater. Sci. 56 (2011) 175–287.
[9] C. Ma, D. Moore, J. Li, Z.L. Wang, Nanobelts, nanocombs, and nanowindmills of wurtzite ZnS, Adv. Mater. 15 (2003) 228–231.
[10] C.-H. Lai, M.-Y. Lu, L.-J. Chen, Metal sulfide nanostructures: synthesis, properties and applications in energy conversion and storage, J. Mater. Chem. 22 (2012) 19–30.
[11] T. Hirate, T. Ito, M. Hikasa, A new multicolor electroluminescent device, J. Appl. Phys. 57 (1985) 976–977.
[12] A.N. Krasnov, P.G. Hofstra, Effect of carrier trapping time on performance of alternating-current thin-film electroluminescent devices, J. Appl. Phys. 90 (2001) 2243–2246.
[13] A.N. Krasnov, Selection of dielectrics for alternating-current thin-film electroluminescent device, Thin Solid Films 347 (1999) 1–13.
[14] M.H. Asghar, F. Placido, S. Naseem, Reactively evaporated multilayer antireflection coatings for Ge optical window, J. Phys. D: Appl. Phys. 40 (2007) 2065–2070.
[15] W. Park, K. Yasuda, B.K. Wagner, C.J. Summers, Y.R. Do, H.G. Yang, Uniform and continuous Y_2O_3 coatings on ZnS phosphors, Mater. Sci. Eng. B76 (2000) 122–126.
[16] R.N. Sharma, A.C. Rastogi, Compositional and electronic properties of chemical-vapor-deposited Y_2O_3 thin film-Si(100) interfaces, J. Appl. Phys. 74 (1993) 6691–6702.
[17] J.J. Chambers, G.N. Parsons, Yttrium silicate formation on silicon: Effect of silicon preoxidation and nitridation on interface reaction kinetics, Appl. Phys. Lett. 77 (2000) 2385–2387.
[18] B.W. Busch, J. Kwo, M. Hong, J.P. Mannaerts, B.J. Sapjeta, W.H. Schulte, E. Garfunkel, T. Gustafsson, Interface reactions of high-k Y_2O_3 gate oxides with Si, Appl. Phys. Lett. 79 (2001) 2447–2449.
[19] K. Kita, A. Toriumi, Origin of electric dipoles formed at high-k/SiO_2 interface, Appl. Phys. Lett. 94 (2009) 132902.
[20] D. Niu, R.W. Ashcraft, Z. Chen, S. Stemmer, G.N. Parsons, Electron energy-loss spectroscopy analysis of interface structure of yttrium oxide gate dielectrics on silicon, Appl. Phys. Lett. 81 (2002) 676–678.

[21] D.-G. Lim, D.-J. Kwak, J. Yi, Improved interface properties of yttrium oxide buffer layer on silicon substrate for ferroelectric random access memory applications, Thin Solid Films 422 (2002) 150–154.
[22] L. Tarnawska, A. Giussani, P. Zaumseil, M.A. Schubert, R. Paszkiewicz, O. Brandt, P. Storck, T. Schroeder, Single crystalline Sc_2O_3/Y_2O_3 heterostructures as novel engineered buffer approach for GaN integration on Si (111), J. Appl. Phys. 108 (2010) 063502.
[23] H.S. Yang, J.W. Kim, G.H. Park, C.S. Kim, K. Kyhm, S.R. Kim, K.C. Kim, K.S. Hong, Interfacial effect on thermal conductivity of Y_2O_3 thin films deposite Al_2O_3, Thermochim. Acta 455 (2007) 50–54.
[24] A.P. Ehiasarian, J.G. Wen, I. Petrov, Interface microstructure engineering by high power impulse magnetron sputtering for the enhancement of adhesion, J. Appl. Phys. 101 (2007) 054301.
[25] H.Y. Zhang, L. Jin, B. Song, J.C. Han, G.G. Wang, X.P. Kuang, R. Sun, Enhancement in hardness and transmittance of ZnS via SiO_2/Y_2O_3 multilayer, J. Alloys Compd. 539 (2012) 40–43.
[26] F. Yan, Z.T. Liu, W.T. Liu, The preparation and properties of Y_2O_3/AlN anti-reflection films on chemical vapor deposition diamond, Thin Solid Films 520 (2011) 734–738.
[27] M. Watanabe, E. Kondoh, Improvement of adhesion and interfacial diffusion behavior in Cu/glass structures using OsO_x layers for microelectromechanical systems, Microelectron. Eng. 120 (2014) 59–66.
[28] P. Lei, J.Q. Zhu, Y.K. Zhu, C.Z. Jiang, X.B. Yin, Evolution of composition, microstructure and optical properties of yttrium oxide thin films with substrate temperature, Surf. Coat. Technol. 229 (2013) 226–230.
[29] J.G. Tao, M. Batzill, Y2O3 Ultrathin, (111) films on Pt (111) substrates, Surf. Sci. 605 (2011) 1826–1833.
[30] E.J. Rubio, V.V. Atuchin, V.N. Kruchinin, L.D. Pokrovsky, I.P. Prosvirin, C.V. Ramana, Electronic structure and optical quality of nanocrystalline Y_2O_3 film surfaces and interfaces on silicon, J. Phys. Chem. C 118 (2014) 13644–13651.
[31] P. Lei, J.Q. Zhu, Y.K. Zhu, C.Z. Jiang, X.B. Yin, Yttrium oxide thin films prepared under different oxygen-content atmospheres: microstructure and optical properties, Appl. Phys. A 108 (2012) 621–628.
[32] M.C. Salvadori, F.S. Teixeira, W.W.R. Araújo, L.G. Sgubin, I.G. Brown, Interface tailoring for adhesion enhancement of diamond-like carbon thin films, Diam. Relat. Mater. 25 (2012) 8–12.
[33] S. Noda, H. Doi, N. Yamamoto, T. Hioki, J. Kawamoto, O. Kamigaito, Improvement for adhesion of thin metal films on ceramics by ion bombardment and the application to metal-ceramic joining, J. Mater. Sci. Lett. 5 (1986) 381–383.
[34] I.V. Mitchell, G. Nyberg, R.G. Elliman, Enhancement of thin metallic film adhesion following vacuum ultraviolet irradiation, Appl. Phys. Lett. 45 (1984) 137–139.
[35] B.N. Chapman, Thin-film adhesion, J. Vac. Sci. Technol. 11 (1974) 106–113.